Ukrainian Journal of Remote Sensing
journal homepage: www.ujrs.org.ua

https://doi.org/10.36023/ujrs.2025.12.4.289

УДК 528.88

Effectual radar satellite monitoring of the initial stages of sandstorm formation and progress in the Sahara Desert

O. Ya. Matveev, https://orcid.org/0000-0003-4811-1191
S. A. Velichko*, https://orcid.org/0000-0002-2579-2134
V. N. Tsymbal, https://orcid.org/0000-0001-9111-0085
D. M. Bychkov, https://orcid.org/0000-0002-1557-7174
V. K. Ivanov, https://orcid.org/0000-0001-5264-9440
O. M. Stadnyk, https://orcid.org/0000-0002-6952-6380

O. Ya. Usikov Institute for Radiophysics and Electronics of the National Academy of Sciences of Ukraine, Acad. Proskura St., 12, Kharkov, 61085, Ukraine

The article is devoted to the elaboration and possibilities of using the method of stage-by-stage satellite radar monitoring of aeolian processes as sources of sandstorms in the process of their growth. The method is based on an experimental study of the effect of anomalous narrow-directional backscattering of radio waves (ANDBR) from an electrically conductive layer formed under the action of the wind, bordering the surface of the barchan. The causes of the formation of such a layer are described, taking into account the physics of the interaction of negatively charged particles when they collide with the surface and with each other in the air. A modified model of combined facet backscattering (MMCFB) by leeward slopes of barchans and ripples located on windward and leeward slopes of barchans is proposed. It should be noted that the angles of these slopes, being the angles of repose of sand, remain constant under radar irradiation at any wavelength. As a result, a comprehensive monitoring of sandstorm characteristics is proposed, during all stages of their passage, using the processing of data from groups of radar satellites operating at the same or different wavelengths. For such type of monitoring, the overall range of surface irradiation angles is also not significant and such fast-passing processes as erosion, evaporation, etc. are excluded from consideration. The obtained data after statistical processing can be compared with field measurement data. The manifestations of the first stages of sandstorm occurrence in fragments of radar images have been confirmed and explained. Prospects for studying the development of storms at the next stages are proposed.

Keywords: radar remote sensing, desert sandstorm monitoring, stages of sandstorm research, complex radar monitoring.

1. Introduction

Sandstorms are one of the global processes that actively influence the Earth's climate, its ecology, human life and health. The dust-sand mixture (DSM) raised into the atmosphere during storms, under the influence of the wind, covers vast regions, crosses the ocean, thereby heating the atmosphere and cooling the earth's surface. When sedimented, DSM accelerates the melting of snow masses and glaciers, changes the geomorphology of the planet, leading to the erosion of rocks and soil, the formation of heterogeneities on the surface of deserts in the form of sand ripples, barchans, dunes, etc.

The scale of the processes, the dynamics of changes in their parameters and their interaction make it difficult to create a generalized theory of sandstorm formation and require new theoretical and experimental research. By now, a number of models of the influence of wind on the main parameters of DSM transportation into the atmosphere have already been developed, tested and adjusted based on data from in-situ measurements. Instrumentation (in the form of wind tunnels) has also been created to test them and monitor sandstorms. (Zhaohui et al., 2012; Bagnold, 1941; Chepil, 1956; Belly, 1962; Jianhua et al., 2006, Li et al., 2014; Besnard et al., 2022. Cornelis and Gabriels, 2004, Kok and Renno, 2003; Cornelis and Gabriels, 2009).

The experience of using multi-zone optical space-based systems TOMS, METEOSAT, MODIS and their analogues (Herrmann, 1999) for detecting and monitoring the spread of storms in the atmosphere has shown the possibility of

*Corresponding author / Автор для кореспонденції: S. A. Velichko / С. А. Величко / sergey19118@gmail.com

using them only as additional ones, due to the unpredictability of weather changes. Radar monitoring methods developed without using modern knowledge about the mechanisms of radio wave scattering during storms also proved to be ineffective. These scattering mechanisms must take into account the electrical interactions of quartz sand particles in surface–particle, particle–particle systems (Stephen & Long, 2005). The paper describes the physics of aeolian processes occurring at all stages of sandstorm development and the possibilities of operational analysis of these processes based on the results of satellite radar monitoring.

2. Preliminary results

Previously, we presented the results of detecting the effects of anomalously narrow-directional backscattering of radio waves (ANDBR) on radar images (RI) of the deserts of Mauritania (part of the Sahara Desert) at practically the same angles of local irradiation of the surface Θ~30º. These are the results of monitoring obtained by both the SLRAR of satellites "Cosmos-1500", "Sich-1" (working wavelength $\lambda = 3.15$ cm), and ASAR Envisat-1 ($\lambda = 5.6$ cm). Note that this effect was observed (see Fig. 1a, c) with opposite wind directions and radar irradiation at different radio wave lengths, by different radars and with a high normalized radar cross-section of barchans $\sigma^0 \leq 6$ dB (Ivanov, et al., 2016, Matveev, et al., Ivanov (Eds.) (2018), Matveev, et al., 2023).

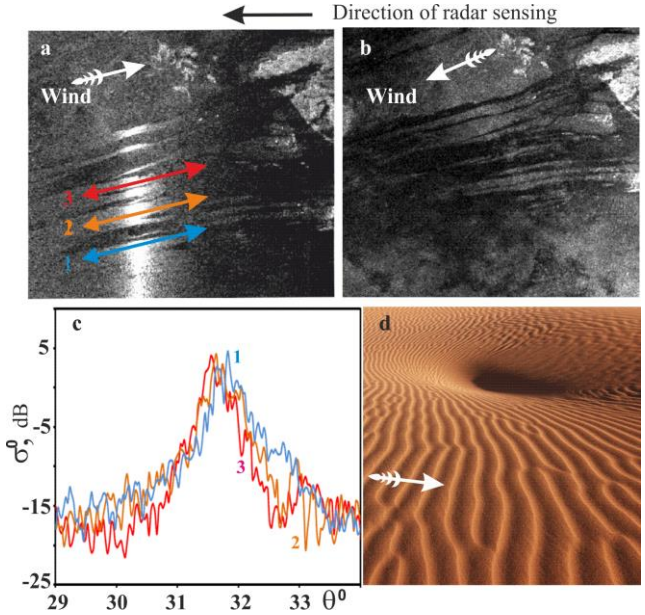

Fig. 1. **a**, **b** – manifestation of the effects of the ANDBR on fragments of the Envisat-1 radar images (Ivanov, et al., 2016; Matveev, et al., Ivanov (Eds.), 2018; Matveev, et al., 2023) ASA_GM1_1P20050112, ASA_GM1_1P20041226 of low resolution 1000x1000 m (©ESA) with opposite directions of wind and radar imaging (left) and with coinciding directions (right); **c** – dependence σ^0 on the azimuthal angle of incidence of the radio wave θ^0, based on the results of processing the sections of the fragment in Fig. 1a; **d** – optical image of a barchan in the deserts of Mauritania. White arrows indicate the wind direction.

Moreover, when the mutual directions of wind and radiation changed by ±45º, σ^0 for ANDBR decreased by no more than 10–20%. Since, according to our estimates, the intensity of radio wave scattering by sand in desert conditions did not exceed $\sigma^0 \sim -14$ dB ÷ –17 dB (Ivanov et al. 2016), it was shown that the most likely mechanism of ANDBR is the scattering of radio waves by a layer of saltons and reptons, which acquire their charge under the action of the wind after breaking away from the surface and colliding with charged particles and dust (Matveev et al., 2023, Kok et al., 2012). The increase in the number of charged particles in the layer creates a growing electric field, which holds the charged particles near the surface and forms a highly conductive layer from them, capable of effectively reflecting radio waves. The ANDBR satellite monitoring technique can already be used for operational monitoring of the initial stages of storms using X-, C- and L-band radars. Moreover, the above-mentioned non-critical mutual deviations in wind directions and radar irradiation make it possible to form groups of different space-based radars and other devices for the duration of a storm for comprehensive storm monitoring.

3. Physics of surface formation processes during sandstorms

We will show that the reason for the large difference (~20 dB) in the values of estimates of the normalized radar cross-section of radio waves scattered by dry sand in the desert σ^0 and the data of satellite measurements of the ANDBR on radar images of barchans, lies in the features of the aeolian processes of transporting DSM into the atmosphere.

Let us recall that barchans are usually asymmetrical crescent-shaped (from above) sand formations, 2–15 m high, located perpendicular to the prevailing wind direction. In spatial cross-section, the barchans are represented by a windward slope – long and gentle (10°–15°) with sand ripples on its surface, repeating the shape of the barchan; and a leeward slope – short and steep (32°–35°), which, depending on its size, can also have (see Fig. 1d) ripples on its surface (Velikanov, 1981; Malinovskaya, 2019; Kenneth, Haim, 2009). The top of the barchan is a sharp ridge, in plan with the shape of an arc, and in the direction of the wind, the pointed ends ("horns") protrude forward.

The soil in the Sahara Desert consists mainly of: 'long-lived' dust (20 μm in size), 'short-lived' dust (20 μm – 70 μm) and quartz sand (70 μm – 500 μm) (Nickling and McKenna Neuman, 2009).

In the ergs with barchans of the Mauritanian deserts of El-Juf, Akshar and Tarza (part of the Sahara Desert) that we studied using radar, seasonal north-east trade winds blow almost continuously at a speed of 3–9 m/s. Therefore, the transport of particles by such winds can occur as a result of several processes, depending mainly on the size of the particles in question.

Usually dust settles on larger particles and in weak winds it is either blown into the air ("long-lived" dust) or

in increasing winds it is knocked out of the soil ("short-lived" dust) by sand particles of 70 μm to 500 μm in size. These particles, overcoming the threshold wind shear velocity $u^* = (\tau/\rho)^{1/2}$ (τ is the shear stress in an arbitrary wind layer and ρ is the aerodynamic air density (Besnard, et al., 2022)) break away from the surface, jumping along it in a process called "saltation" (Bagnold, 1941; Shao, 2008), and the particles are saltons. The impact of these saltons on the soil surface can raise a wide range of particle sizes into the air. Indeed, dust particles of 20 μm to 70 μm in size are usually not lifted into the air by the wind because their interparticle cohesive forces are large compared to aerodynamic forces. Instead, these fine particles are ejected from the soil by saltating particle impacts (Gillette, et al., 1974, Shao, et al., 1993). After being ejected, these dust particles, through turbulent oscillations, join the "short-term" or "long-term" dust.

Impacts of saltating particles can also activate larger particles. However, particles with sizes >500 μm usually do not saltate due to their high inertia (Shao, 2008). After a short jump, usually less than a centimeter, they fall to the ground (a process of transportation called "reptation" (Ungar & Haff, 1987). Larger particles may roll or slide across the surface, driven by the impact of saltating particles and wind in a transport process known as 'creep' (Bagnold, 1937). Creep and reptation can account for a significant proportion of the total flux of wind-blown sand (Bagnold, 1937; Namikas, 2003).

Thus, the transfer of soil particles by wind can be conditionally divided into several physical processes, continuously changing into the next one with a change in wind speed and particle size – this is the transfer of "long-term" suspended dust (20 μm in size). 'short-term' dust (20 –70 μm), saltation (70–500 μm), as well as reptation and creep (500 μm and more). Among the listed processes, "saltation" is dominant.

It should not be forgotten that all aeolian processes associated with the transport of particles into the atmosphere are subject to the electrification of these particles when they are torn from the soil and collide with each other in the air. Proposed models of particle electrification (Kok and Lacks, 2009; Lowell and Truscott, 1986), confirmed by many experimental studies (Schmidt, et al., 1998; Zheng, et al., 2003; Inculet, et al., 2006; Forward, et al., 2009), showed that during collisions, smaller particles become negatively charged, while larger ones become positively charged.

The saltation process initiates several processes at once, which ultimately lead to either the formation of "stationary" saltation (Besnard, et al., 2012) or to the formation of sandstorms, the stages of which are described below.

I. Radar observations: Initial stage of a sandstorm (surface wind speed 1–3 m/s).

Already at a wind speed of about ~1 m/s, "long-lived" dust appears above the surface in the form of stripes of electrified dust particles up to 20 μm in size (see Fig. 2a). Such particles are sources of dust aerosols and can travel thousands of kilometers (Gillette & Walker, 1977), actively influencing the environment. This phenomenon is similar to the snow drift in the Northern Hemisphere.

Also, with a weak (~1 m/s) and unstable in direction surface wind (in Fig. 2b, the left part of the combined radar image Envisat-1 ASA_GM1_1P, 2004-06-11), manifestations of the ANDBR effects are observed. And already at a wind speed of ~2 m/s and a wind practically in the opposite direction of the SAR radiation (right part of the combined SAR image Envisat-1 ASA_GM1_1P, 2004-11-12) the effect of anomalous scattering is already noticeable. The lower value of the maximum RCS (~ –1 dB at a radar incident angle of $\theta = 31.50$ in Fig. 2c, e compared to +5 dB in Fig. 1a) evidences a lower surface wind speed at the time of survey.

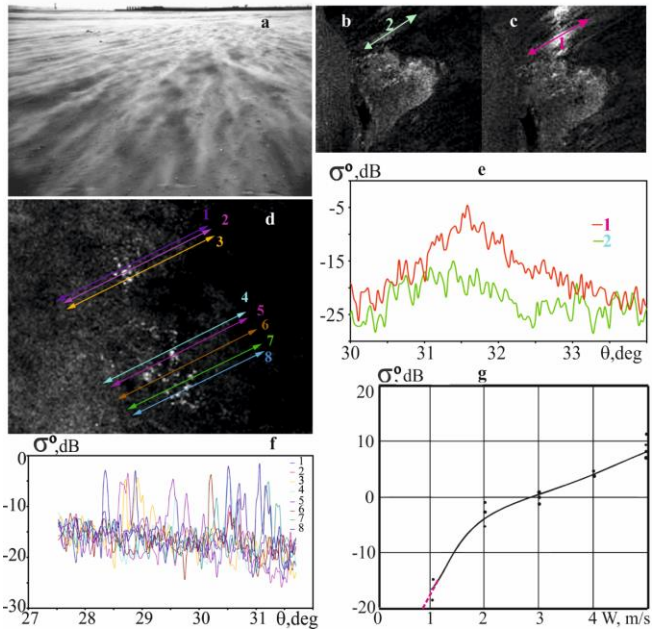

Fig. 2. **a** – photograph of aeolian stripes of "long-lived" dust moving towards the observer (Baas, 2008); **b**, **c** – fragments of radar images (with very light wind – Envisat-1 ASA_GM1_1P 2004-06-11, on the left, and with wind speed of about 2 m/s – Envisat-1 ASA_GM1_1P, 2004-11-12, on the right, © ESA) of the same area of the Akshar desert; **d** – fragment of a radar image (at wind speeds from 1 m/s to 2 m/s – Envisat-1 ASA_ GM1_1P, 2010-14-12, © ESA) of the El Mreie desert area, south of the city of Chinguetti; **e** – graphs of changes σ^0 from the angle of local irradiation θ along the sections of the radar images (Fig. 2 b, c); **f** – graphs of changes σ^0 from the angle of local irradiation θ along the sections of radar images (Fig. 2d); **g** – σ^0 wind dependence (at the ANDBR measurement points) according to the data of (Ivanov, et al., 2016; Matveev, et al., Ivanov (Eds.), 2018); Matveev, et al., 2023), the red dashed line is an approximation of the threshold wind shear speed u^* based on radar data

The incipient stage of the ANDBR effect is also shown in Fig. 2d and 2f. In the radar image fragment (see Fig. 2d, Envisat-1 ASA_GM1_1P, 2010-14-12) bright dots indicate the surface areas where this effect begins to manifest itself. The survey was carried out with a surface wind that was variable in direction relative to the SAR radiation, at a

speed of 1–2 m/s. It should be noted that under these conditions, the narrow backscattering maxima (see Fig. 2f) already reach significant values (–5 dB ÷ –2 dB), but appear in a wider range of angles θ (28.5º ÷ 31.5º) than in the developed state (~31.5º ± 0.25º).

II. Radar observations: Active stage of storm formation (surface wind speed 5÷9 m/s).

The process that begins one of the first is the transformation of sand ripples formed on the surface earlier, and then barchans, by turbulent wind pulsations (Malinovskaya, 2019; Velikanov, 1981; Kenneth, Haim, 2009). In this case, the work (Lämmel, et al., 2012) shows that when a particle hits a surface ("splashes") after a jump, one particle is knocked out of it – the rebound salton, moving at a speed almost equal to the speed of the striking salton. A rebounding salton flies out of the surface at an angle of 34º–40º to the horizon and knocks out up to 20 particles – reptons, depending on the speed and mass of the striking salton (Carneiro, et al., 2013). These reptons move at about one-tenth the speed of a striking salton. Reptons are ejected at an angle of ~70º to the horizon in different directions and begin to accumulate in the near-surface layer at a height of ~3 cm (Steven & Namikas, 2003; Ho, et al., 2014; Greeley, et al., 1996). Reptons are joined by particles of "short-lived" dust knocked out of the surface, 20–70 μm in size (Shao, et al., 1993). As the concentration increases, charged particles create an electric field. The field, in turn, reduces the threshold velocity of particle displacement and increases the number of charged particles in the electrified layer. This process causes an exponential increase in particle concentration (Dur'an, et al., 2011), which leads to an increase in wind drag, thereby slowing the wind speed in the saltation layer (Bagnold, 1936). Such wind slowdown acts as a negative feedback, reducing particle speeds and, in effect, adding new particles to the saltation. It limits the amount of saltating particles (Owen, 1964) to a certain increase in wind speed.

Thus, a layer consisting of negatively charged particles and dust is created above the surface of the barchan. This layer has high conductivity and effectively reflects radio waves. In support of this, analysis of satellite radar images of the Mauritanian deserts (Ivanov, et al., 2016; Matveev, et al., Ivanov (Eds.), 2018; Matveev, et al., 2023) revealed areas of anomalous narrow-directional backscattering of radio waves (ANDBR). In these areas, with opposite wind and radar irradiation directions, σ^0 of the signal received by the radar was 1–2 orders of magnitude greater than the magnitude of the signal received under conditions of corresponding coinciding directions. In the works (Ivanov, et al., 2016; Matveev, et al., 2023) it was concluded that the reason for effective reflection may be an electrified surface layer. This layer repeats the total shape of the barchan and ripple formed by the wind and creates on their windward and leeward slopes a system of reflective quasi-flat areas – reflectors (facets) responsible for the formation of the ANDBR

Taking into account the features of the ANDBR observations and new research data (Malinovskaya, 2019) for the range of surface wind speeds of 5 ÷ 9 m/s, we proposed a modified model of combined facet backscattering (MMCFB) by the leeward slopes of barchans and ripples located on the windward and leeward slopes of barchans (Fig. 1d). In this case, the total RCS σ^0_Σ of the received radar signal can be written as:

$$\sigma^0_\Sigma = \sum_1^b \sigma^0_b + \sum_1^c \sigma^0_{ws} + \sum_1^d \sigma^0_{ls}, \quad (1)$$

where σ^0_b, σ^0_{ws} and σ^0_{ls} are the integral radar cross-sections of signals backscattering from the windward slopes of barchans and ripples on the corresponding windward and leeward slopes of barchans.

This modification of the previously proposed model (Matveev, et al., 2023) follows from our estimates of the influence of processes occurring on the barchan crest on the saltation of particles on the leeward slope of the barchan. In our opinion, at wind speeds of 5 ÷ 9 m/s, the energy of the wind flow swirling toward the surface of the leeward slope of the barchan, despite the visible saturation of the σ^0 of wind dependence curve (Fig. 2g), is only sufficient to sharpen its edge (see Fig. 3). This is confirmed by the fact that the growing electric field in the near-surface layer of the barchan increases the concentration of saltating particles (Dur'an, et al., 2011), which in turn increases wind resistance, actually slowing it down (Bagnold, 1936). The photograph (Fig. 1d) also does not show a noticeable influence on the change in the relief structure of the leeward slope of the barchan.

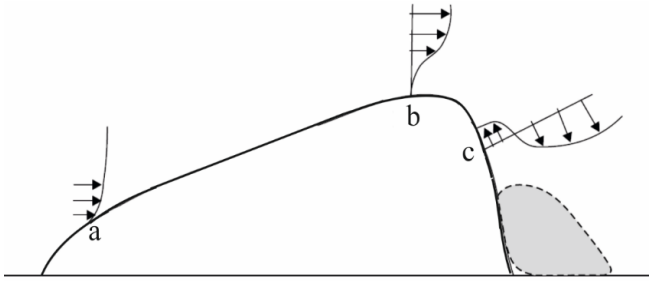

Fig. 3. Change in wind speed profile at the surface of the barchan (Malinovskaya, 2019)

Let us recall that the leeward slopes of the barchans and ripples themselves form an angle with the underlying surface, which is the angle of repose of sand ψ = 30º÷34º (Hamzah M., 2018). The latter depends only on the size of the sand grains, its moisture content and the forces of gravity. Moreover, the range of angles of incidence of the SAR Envisat-1 radio wave is equal to α = 15º÷45º and corresponds to the effective perpendicular reflection of radio waves from the system of reflectors on the slopes of the barchans and makes it possible to promptly monitor the wind dependence σ^0 (see Fig. 2g) and other parameters of aeolian processes.

The model also explains minor changes σ^0 (10% – 20%) when the wind direction changes in the elevation plane relative to the monitoring direction at angles ±45º.

In Fig. 1d it is evident that the leeward slope of the barchan has a crescent shape with a constant slope angle, and the ripples on the windward and leeward slopes are

located in a similar manner (Velikanov, 1981), which explains the weak angular dependence σ^0.

Note that for a more accurate measurement of the threshold wind shear speed u^* using radar data (see Fig. 2g), it is necessary to use more accurate contact data on the direction and speed of weak surface winds.

III. At surface wind speeds of 10÷15 m/s

The length of the saltons' jumps begins to increase and a ripple of 15–30 cm in height begins to form. With that, the number of high-energy particles increases, which the surface electric field is unable to hold. These particles are accelerated by the wind, collide with their own kind, accelerate them, begin the destruction of the surface field, and activate the process of intensifying the storm. In addition, with increasing wind speed, the height of the barchan increases and the difference in pressure at its top (Fig. 3, point b) and in the trough becomes significant. This leads to the formation of an air-sand flow, swirling towards the leeward slope, and the creation of a turbulent vortex, which destroys the relief (ripples) of the leeward slope. The vortex formed by electrified particles weakly reflects radio waves towards the radar. Under the action of the wind, the remaining ripples on the windward slope will also undergo angular distortion, which will significantly reduce its effective scattering surface σ^0. Under such conditions, satellite radar monitoring was not carried out and this work requires additional research.

IV. Stage of maximum storm.

At wind speeds of more than 16 m/s, all sand barchans and ripples are destroyed and a sandstorm develops (Velikanov, 1981; Kenneth, Haim, 2009) with dust and sand grains rising tens and hundreds of meters.

Experimental work at stage IV of the storm requires special equipment. Therefore, work on computer modeling is being carried out around the world (M.V. Carneiro, et al., 2013). However, modeling large processes such as erosion, barchan and dune formation, in which millions of particles interact, taking into account variable winds and other parameters, requires large computational resources.

4. Conclusions

An analysis of the features of the manifestation of the ANDBR effect on the radar images of the ergs of the Mauritanian deserts, together with the data on wind speed, showed that the ANDBR effect is reliably observed with high NRCS ($\sigma^0 \leq 6$ dB), when the directions of the wind speed and radar irradiation vectors are opposite to each other (Fig. 1a). But when the wind and radiation vectors coincided, no effect was observed (Fig. 1b). When the directions of the vectors were misaligned within ±45º, σ^0 was reduced by 10% – 20%.

To explain this effect, in addition to the work of (Matveev, et al., 2023), we proposed a modified model of combined facet backscattering (MMCFB) by the leeward slopes of barchans and ripples located on the windward and leeward slopes of barchans. The latter takes into account the results of additional studies and assessments. The model is based on the influence of the electric field created by electrified particles of a sand-dust mixture saltating under the action of the wind. The field, bordering the surface of the barchan and ripples at a height of ~3 cm, is a highly conductive set of quasi-mirror reflectors of radio waves towards the radar. In this case, the angles of the leeward edges of the barchans and ripples are the angles of repose of sand (natural slope), which depend on the moisture content of the particles, their size and gravitational forces, and do not depend on the wavelength of the radar radiation. The reliability of this scattering model was confirmed by the results of observations of the ANDBR effect by radars at wavelengths of 3 cm and 5.6 cm (Ivanov, et al., 2016, Matveev, et al., Ivanov (Eds.), (2018), Matveev, et al., 2023).

Using the listed features of experimental observation of the ANDBR effect, it is possible to create methods for satellite studies of sandstorms at different stages of their development. Such methods are especially effective when using data from constellations of satellite radars operating at the same or different wavelengths. Studies of this type are not critical to the overall angles of surface irradiation. They help to exclude from consideration such rapidly changing processes as erosion, evaporation, etc. Statistically processed research results can be compared with field measurement data.

Thus, by measuring the effective scattering surface σ^0 at different speeds of the near-surface wind, it is possible to determine the threshold wind shear speed u^*, the speed at which the saturation σ^0 of the sand surface begins at the second stage of storm development, and to study the angular characteristics of the manifestation of the ANDBR.

In addition, the modification of the previously proposed model (Matveev, et al., 2023) is associated with a rethinking of the influence of processes occurring on the leeward slope of the barchan during particle saltation at wind speeds of 4 ÷ 9 m/s (Malinovskaya, 2019). In our opinion, the energy of the wind flow, swirling towards the surface of the leeward slope of the barchan, is only sufficient to sharpen its edge (see Fig. 3). This is confirmed by the fact that the growing electric field in the near-surface layer of the barchan increases the concentration of saltating particles (Dur'an, et al., 2011), which in turn increases wind resistance, actually slowing it down (Bagnold, 1936). The photograph (Fig. 1d) also does not show a noticeable influence on the change in the relief structure of the leeward slope of the barchan.

The actual onset of a sandstorm occurs at surface wind speeds of 10 ÷ 15 m/s. During this process, the number of high-energy particles increases, which the surface electric field is unable to hold. These particles are accelerated by the wind, collide with other particles and speed them up, starting the destruction of the surface field and activating the process of intensifying the storm. Further, with the increase in wind speed, the difference in pressure at the top of the barchan (Fig. 3, point b) and in its trough increases. This leads to the formation of an air-sand flow, swirling towards the leeward slope and the creation of a turbulent

vortex, which destroys the relief (ripples) of the leeward slope. The vortex formed by the electrified particles weakly reflects radio waves towards the radar, which will significantly reduce the overall effective scattering surface σ^0 of the barchan. Under such conditions and at the stage of maximum storm (with wind speeds over 16 m/s), satellite radar monitoring was not carried out and this work requires additional research.

As for testing the modified combined model of radar monitoring of desert areas of the Earth's surface at longer radio waves, additional research is also needed.

The work was carried out using data from a joint project with ESA (C1F. 30193).

Contributions of Authors: Conceptualization – O. Ya. Matveev and S. A. Velichko; methodology – O. Ya. Matveev, S. A. Velichko, V. N. Tsymbal and V. K. Ivanov; formal analysis – O. Ya. Matveev, S. A. Velichko and D. M. Bychkov; investigation – O. Ya. Matveev, S. A. Velichko, D. M. Bychkov and O. M. Stadnyk; data processing – O. Ya. Matveev, S. A. Velichko, D. M. Bychkov and O. M. Stadnyk; writing – original draft preparation: O. Ya. Matveev and S. A. Velichko; writing – review and editing: O. Ya. Matveev. S. A. Velichko, V. N. Tsymbal, V. K. Ivanov, D. M. Bychkov and O. M. Stadnyk; visualization – O. Ya. Matveev and D. M. Bychkov.
All authors have read and agreed to the published version of the manuscript.

Funding: This research received no external funding.

Data Availability Statement: Not applicable.

Acknowledgments: The authors express their sincere gratitude to Earth Observing System Data Analytics (eosda.com) for providing free digital radar images of the Envisat SAR within the framework of the ESA project id:13193. We are also grateful to reviewers and editors for their valuable comments, recommendations, and attention to the work.

Conflicts of Interest: The authors declare no conflict of interest.

Внесок авторів: Концептуалізація – О. Я. Матвєєв та С. А. Величко; методологія – О. Я. Матвєєв, С. А. Величко, В. М. Цимбал та В. К. Іванов; формальний аналіз – О. Я. Матвєєв, С. А. Величко та Д. М. Бичков; дослідження – О. Я. Матвєєв, С. А. Величко, Д. М. Бичков та О. М. Стадник; обробка даних – О. Я. Матвєєв, С. А. Величко, Д. М. Бичков та О. М. Стадник; написання – підготовка авторського рукопису: О. Я. Матвєєв та С. А. Величко; написання – рецензування та редагування: О. Я. Матвєєв, С. А. Величко, В. М. Цимбал, В. К. Іванов, Д. М. Бичков та О. М. Стадник; візуалізація – О. Я. Матвєєв та Д. М. Бичков.
Всі автори прочитали та погодилися з опублікованою версією рукопису.

Фінансування: Це дослідження не отримало зовнішнього фінансування.

Доступність даних: Не застосовується.

Подяки: Автори висловлюють щиру подяку Earth Observing System Data Analytics (eosda.com) за надання безкоштовних цифрових радіолокаційних зображень Envisat SAR в межах проекту ESA з ідентифікатором 13193. Ми також вдячні рецензентам та редакторам за їх цінні коментарі, рекомендації та увагу до роботи.

Конфлікти інтересів: Автори заявляють, що не мають конфлікту інтересів.

References

Baas, A. C. W. (2008). Challenges in aeolian geomorphology. *Investigating Aeolian streamers Geomorphology*, 93, 3–16.

Bagnold, R. A. (1936). The movement of desert sand. *Proc. R. Soc. Lond.*, A 157, 594–620.

Bagnold, R. A. (1941). The Physics of Blown Sand and Desert Barchans. Methuen, New York.

Bagnold, R. A. (1973). Nature of saltation and bed-load transport in water. *Proc. R. Soc. Lond.*, A 332, 473–504.

Belly, P. (1962). Sand movement by wind. *United States army corps of engineers. (Vol. I)*. Coastal Engineering Research Center, Technical Memorandum.

Besnard, J.-B., Dupont, P., El Moctar, A. O. & Valance, A. (2022). Aeolian erosion thresholds for cohesive sand. *Journal of Geophysical Research: Earth Surface*, 127, e2022JF006803. https://doi.org/10.1029/2022JF006803.

Carneiro, M. V., Araújo, N. A. M., Pühtz T. and Herrmann H. J. (2013). Midair collisions enhance saltation arXiv:1212.4603v2 [physics.ao-ph] 8.

Chepil, W. (1956). Influence of moisture on erodibility of soil by wind. *Soil Science Society Proceedings*, 20(2), 288–292. https://doi.org/10.2136/sssaj1956.03615995002000020033x.

Cornelis, W. M. and Gabriels, D. (2003b). The effect of surface moisture on the entrainment of barchan sand by wind: an evaluation of selected models, *Sedimentology*, 50, 771–790. doi: 10.1046/j.1365-3091.2003.00577.

Cornelis, W. M., Gabriels, D. & Hartmann, R. (2004). A conceptual model to predict the deflation threshold shear velocity as affected by near-surface soil water. *Soil Science Society of America Journal*, 68(4), 1154–1161. https://doi.org/10.2136/sssaj2004.1154.

Dong, Z. B. and Qian, G. Q. (2007). Characterizing the height profile of the flux of wind-eroded sediment Environ. *Geol*., 51, 835–45.

Dur´an, O., Claudin, P. and Andreotti, B. (2011). On aeolian transport: grain-scale interactions, dynamical mechanisms and scaling laws. *Aeolian Res*., 3, 243–70.

Ellwood, J.M., Evans, P. D. & Wilson, I. G. (1975). Small scale Aeolian bedforms. *J. Sediment. Petrol*., Vol. 45, 554–561.

Forward, K. M., Lacks, D. J. and Sankaran, R. M. (2009). Charge Segregation Depends on Particle Size in Triboelectrically Charged Granular Materials. *Phys. Rev. Lett*., 102(2), 28001.

Gillette, D. A., Blifford, I. H. and Fryrear, D. W. (1974). The influence of wind velocity on the size distribution of aerosols generated by the wind erosion of soils. *J. Geophys. Res.*, 79, 4068–4075.

Gillette, D. A. and Walker, T. R. (1977). Characteristics of airborne particles produced by wind erosion of sandy soil, high plains of west Texas. *Soil Science*, 123(2), 97–110.

Greeley, R. & Iversen, J. D. (1985). Wind as a Geological Process on Earth, Mars, Venus and Titan. *Cambridge Planetary Science Series* no. 4. xii + 333 pp. Cambridge University Press. ISBN 0 521 24385 8.

Hamzah, M., Beakawi Al-Hashemi, Omar S. Baghabra Al-Amoudi (2018). A review on the angle of repose of granular materials. *Powder Technology*, 330, 397–417. ELSEVIER Publ., https://doi.org/10.1016/j.powtec.2018.02.003.

Herrmann, L., Stahr, K., Jahn, R. (1999). The importance of source region identification and their properties for soil-derived dust: the case of Harmattan dust sources for eastern West Africa. *Contributions to Atmospheric Physics*, 72, 141–150.

Ho, T. D., A. Valance, Dupont, P. A. (2014). Ould El Moctar Aeolian sand transport: Length and height distributions of saltation trajectories. *Aeolian Research*, Vol. 12, March, 65–74.

Inculet, I. I., Castle, G. S. P. and Aartsen G. (2006). Generation of bipolar electric fields during industrial handling of powders. *Chem. Eng. Sci*., 61(7), 2249–2253.

Ivanov, V. K., Matveyev, A. Ya., Tsymbal, V. N., Yatsevich, S. Ye., Bychkov, D. M. (2016). Spaceborne radar identification of desert regions as suppliers of dust into the atmosphere. *Ukrainian Journal of Remote Sensing*. 11. 22–30.

Ivanov, V. K. (Eds.) (2018). Radar monitoring of natural and anthropogenic hazardous phenomena. (Part 2). Lambert Academic Publishing, Germany. Retrieved from https: //www.lappublishing.com.

Jianhua Sun, Linna Zhao, Sixiong Zhao, Renjian Zhang. (2006). An integrated dust storm prediction system suitable for east Asia and its simulation results. *Global and Planetary Change*, 52, 71–87.

Kenneth Pye, Haim Tsoar. (2009). Aeolian Sand and Sand Barchans. Berlin. Heidelberg: Springer.

Kok, J., Renno, F., Nilton, O. (2009). A comprehensive numerical model of steady state saltation (COMSALT), *Journal of Geophysical Research: Atmospheres*, 114, D17, CiteID D17204, September. DOI: 10.1029/2009JD011702.

Kok, J. F., Lacks, D. J. (2009). The triboelectrification of granular systems of identical insulators. *Phys. Rev. E*. In review, available online at http://arxiv.org/abs/0902.3411).

Kok, J. F., Parteli, E. J. R., Michaels, T. I. and Karam, D. B. (2012). The Physics of Wind-Blown Sand and Dust. *Reports on Progress in Physics*, Vol. 75, 106901.

Lämmel M., Rings D. and Kroy K. (2012). A two-species continuum model for aeolian sand transport. *New Journal of Physics*, 14, 093037 (24 pp.). Published 20 September.

Li, B., Ellis, J. T., Sherman, D. J., (2014). Estimating the Impact Threshold for Wind-Blown Sand. In: Green, A. N. and Cooper, J. A. G. (eds.), *Proceedings 13th International Coastal Symposium* (Durban, South Africa), *Journal of Coastal Research*, Special Issue No. 70, 627–632, ISSN 0749-0208.

Lowell, J., Truscott, W. S. (1986). Triboelectrification of identical insulators: II. Theory and further experiments. *J. Phys. D: Appl. Phys.*, 19, 1281–1298.

Malinovskaya, E. A. (2019). Transformation of aeolian relief forms under wind influence. *Izvestiya RAN, Atmospheric and Oceanic Physics*, 53(1), 54–64.

Matveev, A. Ya., Velichko, S. A., Bychkov, D. M., Ivanov, V. K., Tsymbal, V. N. (2023). Modeling of radar scattering by aeolian desert landforms. *Ukrainian Journal of Remote Sensing*, 10(1), 4–10. https://doi.org/10.36023/ujrs.2023.10.1.226.

Nickling, W. G. and McKenna, N. C. (2009). Aeolian sediment transport Geomorphology of Desert Environments ed Parsons, A. and Abrahams, A. D. (pp. 517–555). New York: Springer.

Owen, P. R. (1964). Saltation of uniform grains in air. *J. Fluid Mech*., 20, 225–242.

Schmidt, D. S., Schmidt, R. A., Dent, J. D. (1998). Electrostatic force on saltating sand. *J. Geophys. Res*., 103(D8), 8997–9001.

Shao, Y., Raupach, M. R., Findlater, P. A. (1993). Effect of saltation bombardment on the entrainment of dust by wind, *Journal of Geophysical Research-Atmospheres*, 98(D7), 12719–12726.

Shao, Y. P., Lu, H. (2000). A simple expression for wind erosion threshold friction velocity. *Journal of Geophysical Research-Atmospheres*, 105(D17), 22437–22443.

Shao, Y. P. (2008). Physics and Modelling of Wind Erosion. 2nd edn. (Heidelberg: Springer).

Stephen, H., Long, D. G. (2005). Microwave backscatter modeling of erg surfaces in the Sahara Desert. *IEEE Transactions on Geoscience and Remote Sensing*, 43(2), 238–247.

Steven, L., Namikas, S. L. (2003). Field measurement and numerical modelling of aeolian mass flux distributions on a sandy beach. *Sedimentologym*, 50(2), 303–326.

Ungar, J. E., Haff P. K. (1987). Steady-state saltation in air. *Sedimentology*, 34, 289–299.

Velikanov, M. A. (1981). *Hydrology of land*. L.: Gidrometeoizdat.

Zender, C. S., Bian, H. S., Newman, D. (2003). Mineral Dust Entrainment and Deposition (DEAD) model: description and 1990s dust climatology. *Journal Geophys. Res*., 108, 4416.

Zhaohui Lin, Jason K. Levy, Hang Lei and Michelle L. Bell (2012). Advances in Disaster Modeling, Simulation and Visualization for Sandstorm Risk Management in North China, *Remote Sens.*, 4, 1337-1354. doi:10.3390/rs4051337.

Zheng, X. J., Huang, N., Zhou, Y.-H. (2003). Laboratory measurement of electrification of wind-blown sands and simulation of its effect on sand saltation movement. *Journal Geophys. Res*., 108(D10), 4322. doi:10.1029/2002JD002572.

ЕФЕКТИВНИЙ РАДІОЛОКАЦІЙНИЙ СУПУТНИКОВИЙ МОНІТОРИНГ ПОЧАТКОВИХ СТАДІЙ ФОРМУВАННЯ ТА РОЗВИТКУ ПІЩАНИХ БУР У ПУСТЕЛІ САХАРА

О. Я. Матвєєв, https://orcid.org/0000-0003-4811-1191
С. А. Величко*, https://orcid.org/0000-0002-2579-2134
В. М. Цимбал, https://orcid.org/0000-0001-9111-0085
Д. М. Бичков, https://orcid.org/0000-0002-1557-7174
В. К. Іванов, https://orcid.org/0000-0001-5264-9440
О. М. Стадник, https://orcid.org/0000-0002-6952-6380
Інститут радіофізики та електроніки ім. О. Я. Усикова НАН України, вул. Акад. Проскури, 12, Харків, 61085, Україна

Стаття присвячена розробленню та перспективам використання методики поетапного супутникового радіолокаційного моніторингу еолових процесів як джерел піщаних бур під час їх розвитку. Методика заснована на експериментальному вивченні ефекту аномального вузькоспрямованого зворотного розсіювання радіохвиль від сформованого під дією вітру електрично провідного шару, який облягає поверхню бархану. Описані причини появи такого шару з урахуванням фізики взаємодії негативно заряджених частинок при зіткнення з поверхнею та один з одним у повітрі. Запропонована модифікована модель комбінованого фацетного зворотного розсіювання (ММКФОР) підвітряними схилами барханів та брижів, що знаходиться на навітряних і підвітряних схилах барханів. Оскільки кути цих схилів, що є кутами природного схилу, не залежать від довжини радіолокаційного опромінення, запропоновано комплексний моніторинг характеристик піщаних бур на час усіх етапів їх проходження за допомогою тимчасово створених груп радіолокаційних супутників, що працюють на однакових чи різних довжинах хвиль. Такий моніторинг також не критичний до кутів опромінення поверхні та виключає з розгляду такі швидкоплинні процеси, як ерозія, випаровування та ін. Отримані дані після статистичного оброблення можуть порівнюватися з

даними польових вимірів. Прояви перших етапів виникнення піщаних бур підтверджені та пояснені фрагментами радіолокаційних зображень. Запропоновано перспективи дослідження розвитку бур на наступних етапах.
Ключові слова: радіолокаційне дистанційне зондування, дослідження піщаних бур на різних етапах розвитку, комплексний радіолокаційний моніторинг пустелі,

Рукопис статті отримано 21.08.2025
Надходження остаточної версії: 28.11.2025
Публікація статті: 30.12.2025
Received 21.08.2025
Revised 28.11.2025
Accepted 30.12.2025